ELSEVIER

Journal of Molecular Catalysis A: Chemical 194 (2003) 211–225

JOURNAL OF MOLECULAR CATALYSIS A: CHEMICAL

www.elsevier.com/locate/molcata

Magnetic properties and oxidation state of iron in bimetallic Pt-Fe/KL zeolite catalysts

Thorsten Schmauke [a], Michael Menzel [b], Emil Roduner [a,*]

[a] *Institute of Physical Chemistry, University of Stuttgart, Pfaffenwaldring 55, D-70569 Stuttgart, Germany*
[b] *Federal Institute for Materials Research and Testing (BAM), Richard-Willstätter-Straße 11, D-12489 Berlin, Germany*

Received 8 July 2002; accepted 30 August 2002

Abstract

In view of an understanding of catalytic efficiency the electronic and magnetic state of iron in Fe/KL and the influence of Pt on these properties in Pt-Fe/KL were investigated by superconducting quantum interference device (SQUID) magnetization measurements and Mössbauer spectroscopy. After calcination in air, iron is present only as Fe^{3+} ions in both samples, mainly in a paramagnetic state. There is also a small antiferromagnetic contribution, probably due to iron oxide and hydroxide particles which precipitate on the outer surface of the zeolite crystallites during preparation. After reduction in H_2, the behavior of both samples is predominantly superparamagnetic, but the presence of Pt increases both the saturation magnetization and the size of the residual hysteresis loop. At the same there remains a pronounced paramagnetic contribution which appears to be even slightly higher than before reduction. The interpretation is that alloy particles of metallic Pt–Fe are formed on the outer surface. Since small clusters inside the zeolite crystallites are most active for catalysis the alloy formation seems to be not of relevance for an enhancement of sulfur resistance. It was also shown that during reduction a fraction of Fe^{2+} is formed. The coordination of the Fe^{2+} ions is clearly influenced by Pt and it seems very likely that Fe^{2+} ions are in close contact with Pt clusters. This interaction is probably the origin of the enhanced sulfur resistance and catalytic activity in the reforming reactions.

Keywords: Pt-Fe/KL zeolite; SQUID magnetization measurements; Mössbauer spectroscopy; Oxidation state of iron; Pt–Fe alloy

1. Introduction

Pt/KL was found to be a highly active and selective catalyst for aromatization [1] and also for hydrogenation reactions. Sulfur is a severe poison of metal catalysts because it forms compounds which are strongly chemisorbed on the metal surface [2]. Unfortunately, a mono-functional Pt/KL catalyst shows a much higher sensitivity to sulfur poisoning than the conventional hydrogenation catalyst Pt–Re/Al_2O_3–Cl. This has prevented its application in industry [3]. Vaarkamp et al. [4] and McVicker et al. [5] concluded that the high sensitivity of Pt/KL to sulfur poisoning is attributed to the loss of active surface by adsorption of sulfur compounds and also to the aggregation of small Pt clusters to larger particles which occurs due to the reduced interfacial interactions between neutral Pt clusters and the framework. Simon et al. [6] investigated the sulfur resistance of Pt supported on LTL for benzene hydrogenation.

An improvement of the sulfur resistance of a metal is obtained by a modification of its electronic properties [7]. For example, catalysts containing Lewis acid metals reduce the electron density on the noble metal

* Corresponding author. Tel.: +49-711-685-4490; fax: +49-711-685-4495.
E-mail address: e.roduner@ipc.uni-stuttgart.de (E. Roduner).

1381-1169/02/$ – see front matter
PII: S1381-1169(02)00522-8

by bimetallic interaction [8,9]. In the present case, a better sulfur resistance of Pt/KL is achieved by addition of iron. The effect is ascribed to two different mechanisms: Fe ions (such as Fe^{2+}) act as chemical anchors for the particles during reduction and catalysis, and therefore they prevent the clusters from becoming highly mobile and forming larger aggregates [10,11]. Secondly, in its metallic state, a noble metal is able to dissociate hydrogen. The H atoms can reduce Fe^{3+} or Fe^{2+} ions which are in close contact with the noble metal particle, to Fe(0), which results in alloy formation [12]. In monometallic Fe zeolites there is no H atom formation, and consequently reduction of individual iron ions to the metallic state is known to be more difficult than reduction of bulk Fe_2O_3 particles since iron ions in zeolites are stabilized by framework coordination [13]. In zeolites, the reduction to Fe(0) using hydrogen as reducing agent has been reported to be not possible, so that stronger agents such as Na vapor or NaN_3 are required [14]. However, at temperatures higher than 693 K the reduction to Fe(0) using hydrogen becomes possible [15].

In a recent publication [16] the influence of iron as a co-impregnated second metal component on the decomposition, dispersion and catalysis of the platinum amine complex in KL zeolite was investigated. By XPS it was demonstrated that Pt^{2+} ions migrate into inner sites of KL crystallites during calcination, whereas Fe^{3+} shows a pronounced surface enrichment. It was also shown that the Pt particles are more electron deficient after reduction, owing to the partial electron transfer from Pt to Fe^{+} ions. This effect can also be discussed in terms of the Sanderson electronegativity for solids [17] which states that the electronegativity of a zeolite is the geometric average of the electronegativities of all atoms of the zeolite [18]. In Pt-Fe/KL part of the K^{+} cations are replaced by Fe cations. This increases the electronegativity of the whole system and reduces the electron density on the platinum clusters. As a consequence, the bimetallic Pt-Fe/KL zeolite shows a higher performance on both catalytic activity and sulfur resistance in hydrogenation and aromatization reactions. Fe reduction was clearly enhanced in Pt-Fe/KL compared to monometallic Fe/KL, but it was not possible to decide whether this results in the formation of Fe^{2+}, metallic Fe(0), or a metallic Pt–Fe alloy.

Mössbauer spectroscopy is a sensitive tool for the investigation of the oxidation state of iron. The existence of a chemical isomer shift (IS) produced by different chemical environments was first demonstrated by Kistner and Sunyar [19] in 1960. It was shown that the chemical shift is related to the formal oxidation state of the iron. Another parameter is the magnetic hyperfine interaction of the nucleus with magnetic fields. It is characteristic for the magnetic properties of the sample (i.e. ferromagnetism) [20]. It causes a sextet structure of a spectrum. For nanoparticles the time between two electron spins flips is size dependent and therefore, the hyperfine interaction is partly or completely averaged out [21].

Isomer shifts amount to typically 0.3–0.4 mm s^{-1} for high-spin Fe^{3+} and to 0.7–1.5 mm s^{-1} for Fe^{2+}. For Pt–Fe alloy in zeolite catalysts, Woo et al. [22] found a shift of 0.11–0.16 mm s^{-1} relative to metallic iron, and Kajcsos et al. [23] reported 0.07 mm s^{-1}. These are typical metallic isomer shifts, but there is a controversy in literature about the interpretation of doublet signals with a shift of about 0.3 mm s^{-1} and a quadrupolar splitting in the range 0.6–1.0 mm s^{-1} that were found in diverse catalysts containing a group VIII noble metal and iron. These parameters are normally characteristic of high-spin Fe^{3+}, and several authors [13,24–30] made this assignment in bimetallic catalysts. Other authors like Garten [31], Lam and Garten [32], Vannice et al. [33], and Garten and Sinfelt [34] favor the interpretation that this doublet corresponds to zerovalent iron atoms on the surface of alloy particles. Their conclusions are based on chemical arguments. For example, in the case of Rh-Fe/NaY [35,36] and Pd-Fe/NaY [12], evidence was presented that part of the iron was reduced to the zerovalent state and alloyed to the noble metal, while the remaining fraction was reduced from Fe^{3+} to Fe^{2+}. Lam and Garten [32] explain these high isomer shifts by assuming that the electron density on surface iron atoms is lower than for iron atoms in bulk alloys. Table 1 contains an overview of Mössbauer parameters assigned to Pt–Fe alloys. The situation becomes in addition more complicated by the fact that metallic Fe phases can show doublets or sextets depending on the Fe/Pt ratio, support and temperature.

The two interpretations of the doublet signal near 0.3 mm s^{-1} seem to be somewhat in conflict, and an investigation of the oxidation state of iron in Pt-Fe/KL

Table 1
Overview of Mössbauer parameters found for Pt–Fe phases (isomer shifts relative to metallic α-iron)[a]

Sample	IS ($mm\,s^{-1}$)	QS ($mm\,s^{-1}$)	HF (T)	T (K)	References
Pt-Fe/NaY	0.31	0.55		295	[36]
Pt-Fe/SiO_2	0.28	0.46		295	[28]
Pt–Fe alloy	0.29–0.32		28.8–31.0	300	[37]
Pt-Fe/SiO_2	0.11–0.16	0.22–0.32		523	[22]
Pt-Fe/SiO_2	0.30	0.43		295	[38]
Pt-Fe catalyst	0.348			295	[39]
Pt–Fe	0.28–0.51			298	[40]
Pt–Fe/C	0.305–0.325	0.423–0.987		295	[41]

IS: isomer shift; QS: quadrupole splitting; HF: hyperfine splitting; T: temperature.
[a] IS = 0 $mm\,s^{-1}$, HF = 33.0 T [20].

by another technique is highly desirable. The highly sensitive SQUID magnetization measurements provide information about the magnetic properties of the samples and distinguish between diamagnetic, paramagnetic, antiferromagnetic and ferromagnetic or superparamagnetic states. In many cases the magnetic behavior is a superposition of more than one magnetic property. In our samples, the diamagnetic part is mainly a property of the zeolite framework and should thus be comparable to the diamagnetism of SiO_2. On the other hand, in all common oxidation states (0, +2, +3) Fe bears at least one unpaired electron. Therefore, iron should show either paramagnetic, antiferromagnetic or ferromagnetic magnetization, depending on its oxidation state and dispersion. Ferromagnetic behavior is well known for pure metallic iron or for iron alloys. Fe(II) and Fe(III) oxides are often antiferromagnetic (e.g. in Fe_xO, α-Fe_2O_3) but sometimes also ferromagnetic (e.g. in γ-Fe_2O_3 in the temperature range below 260 K) [42]. As the volume of a ferromagnetic particle is reduced, a size is reached below which the anisotropy energy is smaller than the thermal energy. In that case, thermal fluctuations cause the magnetic moment of the domains to fluctuate randomly between their energy minima; hence the particles behave like a paramagnet [43].

In principle the magnetic behavior of Fe can also be determined by EPR spectroscopy. We performed such measurements in our previous work [16], but a disadvantage is the dependence of the EPR signal intensity on relaxation effects which may be temperature dependent or even field dependent and therefore falsify interpretations. Furthermore, some EPR lines of iron species are very broad. Due to limitations in the magnetic field modulation amplitude and due to baseline drifts continuos wave EPR is not very sensitive to such broad lines. In addition the signal intensity of forbidden transitions which are common for Fe^{3+} depends on the local geometry.

The aim of the present work is to compare results of Mössbauer spectroscopy and SQUID magnetization measurements in order to obtain more clarity concerning the interaction Pt and Fe in bimetallic Pt-Fe/KL catalysts. An answer to this question is a key to a further understanding of the enhanced sulfur resistance of bimetallic Pt-Fe/KL compared with monometallic Pt/KL catalysts.

2. Experimental

2.1. Sample preparation

2.1.1. Preparation of $^{57}Fe(NO_3)_3$

30 mg of ^{57}Fe (Chemotrade, enrichment 95.85%) were dissolved in 5 ml of concentrated HNO_3. The solution was evaporated just to the point before dryness in order to prevent the formation of insoluble iron oxides or hydroxides after prolonged heating. The residue was then dissolved in an adequate amount of water to obtain a 0.0107 M $^{57}Fe(NO_3)_3$ solution [44].

2.1.2. Preparation of Fe/KL and Pt-Fe/KL

KL zeolite (Si/Al = 3.0) was obtained from CU Chemie Uetikon AG. Wet impregnation with 0.0107 M $^{57}Fe(NO_3)_3$ (Aldrich) or $^{57}Fe(NO_3)_3$ was performed at 353 K to yield samples of 0.3 wt.% iron loading. For bimetallic Pt-Fe/KL catalysts, $Fe(NO_3)_3$, or $^{57}Fe(NO_3)_3$, respectively, and *cis*-$Pt(NH_3)_2Cl_2$ were co-impregnated to yield samples of 0.3 wt.%

iron and 1.0 wt.% platinum, giving a 1:1 Fe/Pt atomic ratio (subsequently called Pt-Fe/KL for brevity). The products were dried in vacuum at room temperature and kept in a desiccator. For calcination in a high flow of O_2 (600 ml g^{-1} min^{-1}) in a packed bed reactor the temperature was raised at 0.5 K min^{-1} from room temperature to 573 K where it was kept for 1 h. After purging with N_2, reduction was performed in a H_2 flow (180 ml g^{-1} min^{-1}) while the temperature was raised at 8 K min^{-1} from room temperature again to 573 K and kept at this level for 1 h. Samples were always handled under N_2 in a glove box [16].

2.2. SQUID magnetization measurements

Superconducting quantum interference device (SQUID) magnetization measurements were performed using a Quantum Design MPMS-5S instrument in the −30 to +30 kOe external magnetic field range and the 3–400 K temperature interval. Measurements were performed at constant field varying the temperature or vice versa.

2.3. Mössbauer spectroscopy

In a glove box, samples were sealed into Plexiglas cells. Mössbauer spectra were obtained at 78 and 295 K using conventional spectrometers (CM-2201 and WISSEL) operated in constant acceleration mode. Isomer shifts are reported relative to metallic α-iron. In order to obtain better signal intensities ^{57}Fe enriched samples were used for measurements. Fitting of experimental results was performed with an appropriate number of doublets and sextets. The criteria for selecting best fits and the correct number of peaks were the chisquared value and physically meaningful parameters, e.g. only positive line intensity. Due to large differences in spectra of different samples it was not possible to use a single model to fit all spectra.

3. Results and discussion

3.1. Calcined Fe/KL and Pt-Fe/KL

Mössbauer measurements of Pt-Fe/KL samples, performed at 295 and 78 K, are depicted in Fig. 1,

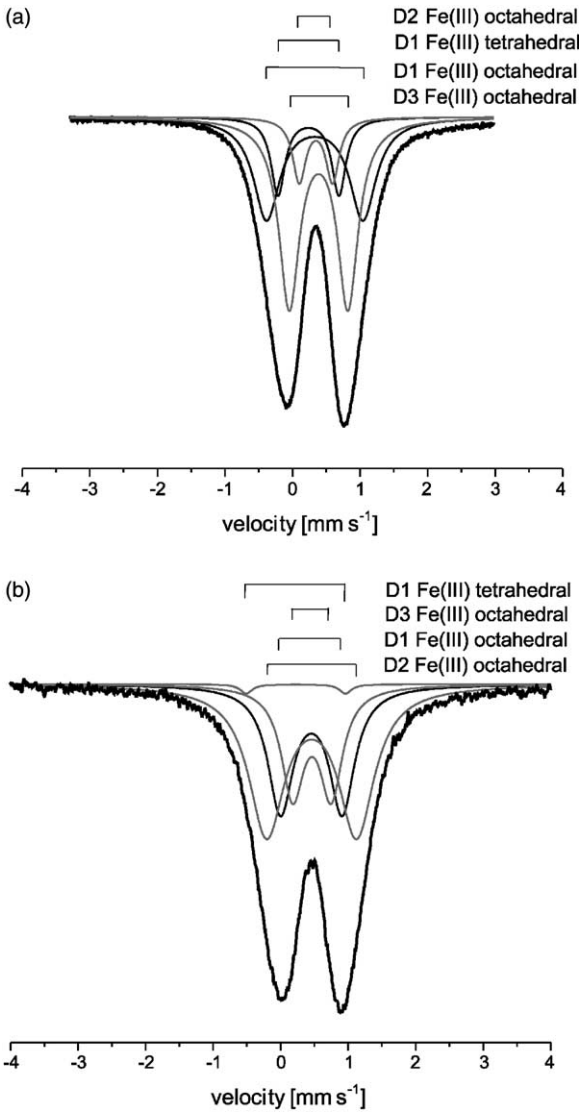

Fig. 1. Mössbauer spectra of calcined 1.0% Pt-0.3% Fe/KL catalyst at (a) 295 K, (b) 78 K.

the Mössbauer parameters are presented in Table 2. Several doublets detected at both temperatures are assigned to tetrahedrally coordinated Fe^{3+} species, and at least three different octahedrally coordinated Fe^{3+} species were detected. Some authors reported that during calcination, the NH_3 ligands of decomposing *cis*-$Pt(NH_3)_2Cl_2$ can bind to any Lewis acidic site in the zeolite and then reduce ions like Pt^{2+} [45,46] or

Table 2
Mössbauer parameters of calcined 1.0% Pt-0.3% Fe/KL at 295 and 78 K and their assignments (D: doublet)

	78 K			295 K		
	IS ($mm\,s^{-1}$)	QS ($mm\,s^{-1}$)	Signal area (%)	IS ($mm\,s^{-1}$)	QS ($mm\,s^{-1}$)	Signal area (%)
D1 Fe(III) tetrahedral	0.23	1.47	1.03	0.24	0.90	12.86
D1 Fe(III) octahedral	0.45	0.91	28.74	0.33	1.43	31.56
D2 Fe(III) octahedral	0.46	1.33	47.93	0.35	0.49	9.99
D3 Fe(III) octahedral	0.46	0.57	22.30	0.39	0.87	45.59

IS: isomer shift; QS: quadrupole splitting; HF: hyperfine splitting.

Fe^{3+} [16,47]. In our samples, isomer shifts typical for Fe^{2+} ions were not found, giving no evidence for reduction of Fe^{3+} by the NH_3 ligands during calcination. In a recent publication we reported that the EPR signal at $g = 2.3$ gains in intensity during reduction, and we interpreted this also in terms of partial reduction of Fe^{3+} ions [16]. Taking our present results into account, it can be concluded that in calcined Pt-Fe/KL the Pt^{2+} ions are located near Fe^{3+} ions and therefore influence the signal intensity. However, our present results do not exclude that autoreduction occurs, because Fe^{2+} ions would be easily reoxidized during calcination. The accidental oxidation of Fe^{2+} ions in reduced Fe/KL and Pt-Fe/KL samples in Mössbauer cells which were not completely sealed (see Sections 3.2 and 3.3) seems to support this suspicion.

Magnetization measurements of Fe/KL and Pt-Fe/KL catalyst samples were performed at constant field (1 and 10 kOe) versus temperature (Fig. 2). Because commercially available zeolites always contain small amounts of iron impurities, magnetization measurements were performed as well on untreated KL zeolite in order to take such iron impurities into account.

In first approximation the magnetization behavior of all three samples (calcined Fe/KL and Pt-Fe/KL; untreated KL) is paramagnetic, but there are additional magnetic contributions.

The small shift in the susceptibility curves between 1 and 10 kOe indicates the presence of small amounts of ferromagnetic compounds in the calcined Fe/KL and Pt-Fe/KL samples (Fig. 3), because the ferromagnetic saturation magnetization is the

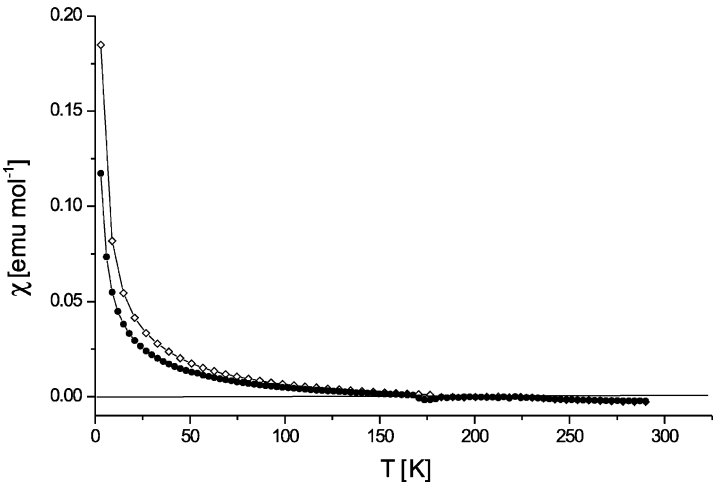

Fig. 2. Molar magnetic susceptibility (with respect to the molar amount of iron) vs. temperature at 10 kOe: (◇) calcined 1.0% Pt-0.3% Fe/KL, (●) calcined 0.3% Fe/KL. The curves are obtained from field cooled measurements. The magnetization of 1.0% Pt-0.3% Fe/KL is only slightly higher than for calcined 0.3% Fe/KL indicating that the oxidation state of iron must be the same.

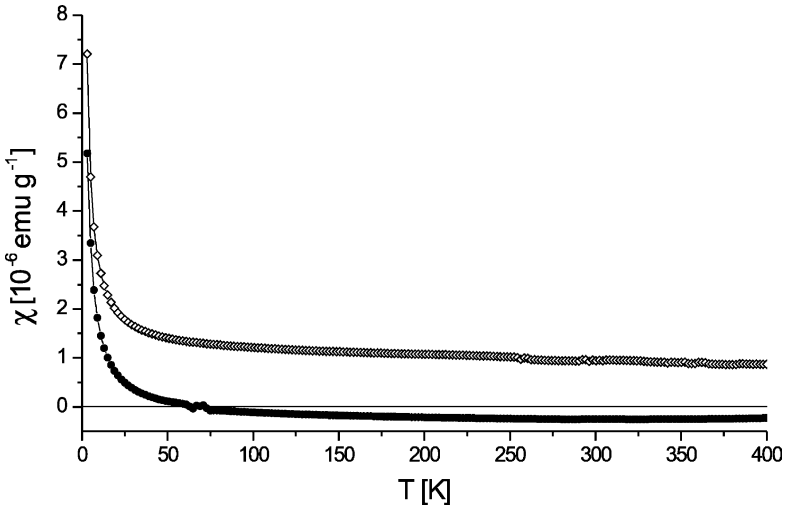

Fig. 3. Mass magnetic susceptibility (with respect to the zeolite mass) vs. temperature at 1 kOe (◇) and 10 kOe (●) for untreated KL. The curves are obtained from field cooled measurements. Note that the *Y*-axis shows the molar magnetization divided by the magnetic field, thus without ferromagnetic contribution there should be no shift between curves measured at different magnetic fields.

only contribution that is independent of the applied magnetic filed. The ferromagnetic magnetization corresponds to only 7.5 ppm (related to α-iron with a mass equivalent to the zeolite mass) of the saturation magnetization of metallic iron. Since the same shift between the susceptibility curves for 1 and 10 kOe is also present in magnetization curves of untreated KL zeolites, this feature should be attributed to a ferromagnetic impurity (small amounts of iron are present in all commercially available zeolites), but not to iron introduced into the zeolite by impregnation. It is, therefore, not investigated in more detail.

In high fields, the temperature dependence of the magnetization of the samples was fitted by the theoretical suceptibility χ (T) that includes paramagnetism, diamagnetism and ferromagnetic saturation magnetization: $\chi\,(T) = C/(T-\Theta) + \chi_{\mathrm{dia}} + M_{\mathrm{sat}}/H$ (C: Curie constant, χ_{dia}: diamagnetic susceptibility, M_{sat}: ferromagnetic saturation magnetization, H: magnetic field). The diamagnetic susceptibility of untreated KL amounts to -0.62×10^{-6} emu g^{-1} and is in good agreement with that expected for SiO_2 (-0.49×10^{-6} emu mol^{-1}). The chisquared values for the susceptibility fits of calcined Fe/KL and Pt-Fe/KL are larger than for untreated KL even though there was no serious systematic deviation. Small additional magnetic contribution may be responsible for these deviations. The effective magnetic moments for Fe^{3+} derived from the Curie constants (Table 3) are about a factor 2–3 below the value of 5.9 μ_B ($\mu = g\,[s(s+1)]^{1/2}\,\mu_B$) that is expected for high-spin Fe^{3+} ions, where g is the g-value of the unpaired electrons in the system. As in EPR measurements [16] the effective magnetic moment of Fe^{3+} in Pt-Fe/KL is larger than in Fe/KL due to the influence of Pt^{2+} ions in the neighborhood of Fe^{3+} ions. The increase of the effective magnetic moment of Fe^{3+} is partly due to an increase of the g-value that is caused by the additional coupling of the electron spin moment of Fe^{3+} with the orbital moment of Pt^{2+}. On the other hand it seems also possible that this may only reflect the limits of reproducibility of sample preparation. Low spin Fe^{3+} carries a lower magnetic moment, but due to the weak ligand fields of the water, hydroxide or framework oxygen ligands only the high-spin ferric state is expected in zeolites [48], and the reduced magnetic moment must be a result of partial antiferromagnetic coupling between Fe^{3+} ions that results in canceling of magnetic moments. Another argument supporting the antiferromagnetic contribution is the small negative value for Θ (−3 K) that is obtained for a fit of the $1/\chi$ curve by the Curie Weiss law. The most common antiferromagnetic iron oxide is α-Fe_2O_3 (hematite), but the absence of a hyperfine

Table 3
Magnetic parameters of investigated samples

	Untreated KL	Calcined		Reduced	
		Fe/KL	Pt-Fe/KL	Fe/KL	Pt-Fe/KL
C (emu K mol^{-1})	[a]	0.72[b]	0.94[b]	0.88[c]	1.08[c]
P_{eff} (μ_B)	–	2.39	2.73	2.64	2.93
M_{sat} (emu mol^{-1})	–	–	–	1543[c]	6447[c]
M_{sat}/M_{sat} (bulk) at 50 K	7.5×10^{-6}[d,e]	7.5×10^{-6}[d,e]	7.5×10^{-6}[d,e]	0.13[e]	0.34[f]
M_{rem} (emu mol^{-1}) at 50 K	–	–	–	375	2600
H_{coerc} (Oe) at 50 K	–	–	–	300	750
C_{dia} (emu g^{-1})	-0.62×10^{-6}[g]	[g]	[g]	[g]	[g]

C: Curie constant; χ_{dia}: diamagnetic susceptibility; M_{sat}: ferromagnetic saturation magnetization; H: magnetic field; p_{eff}: effective magnetic moment; M_{rem}: remanent magnetization; H_{coerc}: coercive field.

[a] The Curie constant of untreated KL zeolite is $C = 2 \times 10^{-5}$ emu K g^{-1} and is related to the entire sample mass. The exact amount of iron impurities in KL zeolite is not known.

[b] Obtained from a fit of $\chi(T) = C/(T - \Theta) + \chi_{dia} + M_{sat}/H$ (M_{sat} was determined as described in footnote d).

[c] Obtained from a fit of $M(H) = M_{sat} + HC/T$ (for $H > 10000$ Oe).

[d] M_{sat} was obtained from the displacement of the χ (T) curves obtained at 1000 and 10,000 Oe. For untreated and calcined samples it is related to the zeolite mass since it is a property of iron impurities in commercially available zeolites and the exact amount of iron impurities is unknown.

[e] Relative to 12,286 emu mol^{-1} for bulk α-iron [47].

[f] Relative to 19,100 emu mol^{-1} for bulk Pt–Fe (1/1 atomic ratio).

[g] Related to the zeolite mass and assumed to hold for all samples.

sextet in Mössbauer spectra does not support the presence of significant amounts of bulk antiferromagnetic α-Fe_2O_8. However, for particles of α-Fe_2O_3 of the order of 5.0–7.5 nm in diameter or life time of an excited Mössbauer state (10^{-8} s) and as a consequence the magnetic hyperfine interaction is averaged out, and the iron appears paramagnetic in the Mössbauer spectrum [21]. A quadrupole doublet can therefore be indicative of small α-Fe_2O_3 particles, because the hyperfine interaction is averaged out.

In conclusion, all iron in calcined Fe/KL and Pt-Fe/KL is present as Fe^{3+}, partly located on cation sites inside the zeolite crystallites where they substitute K^+ ions. These Fe^{3+} ions do not interact with each other, and therefore their behavior is paramagnetic. This part of the iron is corresponding to iron ions dispersed atomically or as very small aggregates in the channels of the zeolite. The rest of the Fe^{3+} ions forms antiferromagnetic oxides, probably α-Fe_2O_3 (hematite) located mostly at the outer surface of the zeolite crystallites. Due to their small size these particles appear to be paramagnetic in Mössbauer spectroscopy. During impregnation of KL with a $Fe(NO_3)_3$ solution the introduction of Fe ions or oxide or hydroxide particles into the zeolite takes place, but in addition precipitation of isolated Fe_2O_3 particles occurs during impregnation when the pH value of the $Fe(NO_3)_3$ solution is too high to prevent the formation of colloidal iron oxide or hydroxide particles.

The final parameter to consider is the Mössbauer spectral area that can sometimes give information about the relative amount of different iron species. However, its dependence on lattice dynamics can complicate composition analysis, particularly in view of the fact that the Debye temperature of Mössbauer surface atoms can be as low as half of the Debye temperature for bulk atoms [21]. As a consequence, spectral areas of different iron species show different temperature dependencies because the recoilless fraction of γ-quantum absorption depends on the ratio between experimental temperature and Debye temperature. For calcined as well as for reduced Fe/KL, the relative spectral areas are indeed temperature dependent. Thus, they provide primarily information about the strength of bonding of the Mössbauer atom to the solid matrix rather than about the sample composition. However, a rough estimation of the contribution of different Fe species is still possible.

Table 4
Mössbauer parameters of reduced 0.3% Fe/KL at 295 and 78 K and their assignments (D: doublet, S: sextet)

	78 K				295 K			
	IS ($mm\,s^{-1}$)	QS ($mm\,s^{-1}$)	HF (T)	signal (%)	IS ($mm\,s^{-1}$)	QS ($mm\,s^{-1}$)	HF (T)	signal (%)
D1 Fe(III) octahedral	0.46	0.91		21.96	0.35	0.66		25.92
D2 Fe(III) octahedral	0.59	2.69		33.93	0.34	1.12		45.94
D3 Fe(II) octahedral					1.14	1.55		10.20
S1 Fe(0) metal	0.12	−0.0004	34.3	9.38	0.01	0.01	32.9	13.90
S2 Fe partially oxidized	0.54	−0.10	47.4	7.84	0.21	−0.31	34.6	4.04
S2 Fe(III) compensation sextet	0.46	−0.01	39.6	26.89				

IS: isomer shift; QS: quadrupole splitting; HF: hyperfine splitting.

3.2. Reduced Fe/KL

Mössbauer spectra of reduced Fe/KL were recorded at 295 and 78 K and are depicted in Fig. 4. Table 4 gives the parameters and assignments of the signals. Doublets of at least two octahedrally coordinated Fe^{3+} phases (distribution of different distorted octahedral sites) were found. In addition, measurements at 295 K indicated the presence of octahedrally coordinated Fe^{2+}, but in later measurements either at 78 K or again at room temperature this phase was not found again. Obviously the Mössbauer cells were not completely sealed, permitting slow oxidation of Fe^{2+} to a phase with an oxidation number between +2 and +3 for Fe. This partly oxidized phase is characterized by a sextet with parameters between those of Fe and Fe_3O_4. Another sextet with an isomer shift of $0.12\,mm\,s^{-1}$ at 78 K and $0\,mm\,s^{-1}$ at room temperature was detected, which clearly has to be assigned to a ferromagnetic phase of metallic iron. As the volume of a ferromagnetic particle is very small, a size may be reached at which the magnetic anisotropy energy is smaller than the thermal energy. In that case, thermal fluctuations cause the magnetic moments of the domains to fluctuate randomly between their energy minima, hence at not too low temperatures the particles behave principally like a paramagnet. Because of the large magnetic moments of the particles, this behavior is called superparamagnetic. The temperature at which anisotropy energy and thermal energy are equal is called “blocking temperature”. In order to appear superparamagnetic in Mössbauer spectroscopy, the fluctuations must be faster than the life time of an excited Mössbauer state that is about 10^{-8} s [43]. In our case the iron phase is also ferromagnetic at room

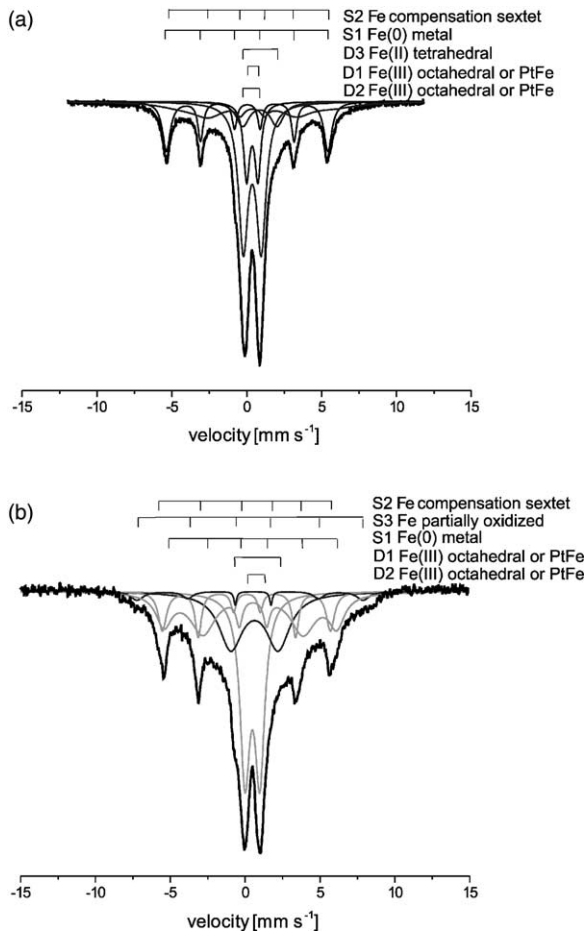

Fig. 4. Mössbauer spectra of reduced 0.3% Fe/KL samples at (a) 295 K, (b) 78 K.

temperature in Mössbauer spectroscopy. At 78 K an additional sextet called here a compensation sextet with an isomer shift of 0.46 mm s^{-1} was found. The lines of this sextet were broad due to a fast electron spin relaxation. The origin of the compensation sextet is not yet clear. Possibly, it represents another partially oxidized Fe phase. A further possibility is that this sextet does not represent a real Fe phase. In this case the other doublets and sextets are not sufficient to describe the phases assigned to them. This means that for example two doublets may be not sufficient to describe Fe^{3+}.

SQUID magnetization measurements performed by varying the temperature at constant field are depicted in Fig. 5, whereas magnetization measurements in dependence of the field at a constant temperature are shown in Fig. 6. The magnetization of reduced Fe/KL and in particular of Pt-Fe/KL samples (see next section) is much higher than for calcined samples, and the behavior is mainly superparamagnetic, since there is only a minor hysteresis loop present. Because of the differences in the measurement time (a few seconds for SQUID and 10^{-8} s for Mössbauer) the blocking temperature for SQUID is lower than for Mössbauer spectroscopy, and consequently phases that behave as ferromagnets in Mössbauer spectroscopy may behave as superparamagnets in SQUID measurements [43]. This superparamagnetic phase is attributed to the metallic iron phase detected also by Mössbauer spectroscopy.

It is surprising to find metallic iron in monometallic Fe/KL samples, since it is generally accepted that in zeolites, Fe ions cannot be reduced to metallic Fe by H_2 in the absence of noble metals. Reduction of Fe ions to metallic Fe is complicated in zeolites due to stabilization of Fe ions by framework oxygen coordination, and therefore stronger reduction reagents like Na vapor are required [14] or higher temperatures are required [15]. It can thus be concluded that metallic iron is either located on the outer surface of the zeolite crystallites or that it exists even as isolated particles. Fe_2O_3 or iron hydroxide particles can be precipitated during impregnation of zeolites with a $Fe(NO_3)_3$ solution due to a too high pH value. In contrast to isolated Fe ions in zeolites, they are easily reducible. The amount of the superparamagnetic saturation magnetization is 1543 emu mol^{-1} (related to Fe) compared to a saturation magnetization of 12,286 emu mol^{-1} for metallic α-iron [49]. It seems therefore reasonable to conclude that about 12% of all iron introduced into the zeolite is reduced to metallic iron, being in good agreement with the amount that can be estimated by Mössbauer spectroscopy (Table 4).

There should be a broad distribution of iron particle sizes, because these particles are not localized in the pore structure of L zeolite, and therefore any

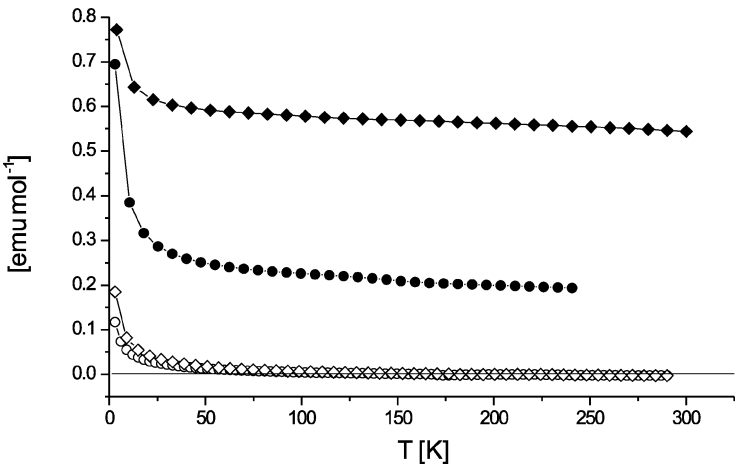

Fig. 5. Molar magnetic susceptibility (with respect to the molar amount of iron) vs. temperature at 10 kOe: (◆) reduced 1% Pt-0.3% Fe/KL, (●) reduced 0.3% Fe/KL. The high magnetization is due to superparamagnetic behavior. Curves from calcined samples are depicted for comparison (lower curves).

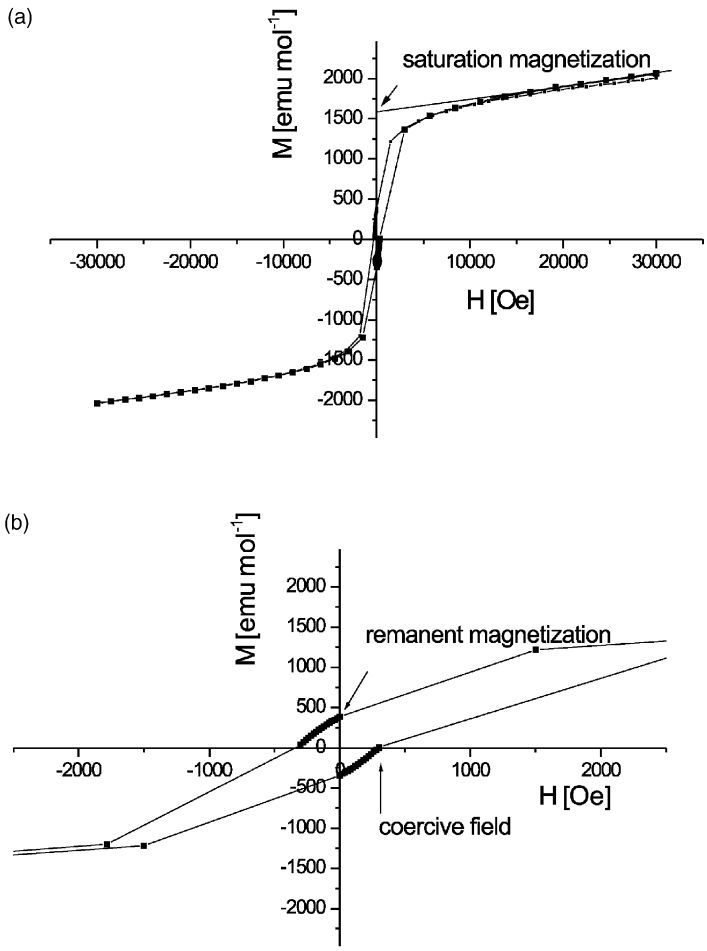

Fig. 6. Molar magnetic susceptibility (with respect to the molar amount of iron) vs. magnetic field at 50 K of reduced 0.3% Fe/KL for the full range (a) and an expanded range (b).

influence of the zeolite framework to prevent particles to grow by sintering is missing. In this way a few particles reach a size that is large enough for ferromagnetic behavior, and the small hysteresis curve that remains should be attributed to these large particles. By comparison of saturation magnetization and coercive field at 50 K with literature values on ultrafine iron particles with oxide shell [43] we estimate a particle diameter of ca. 2.5 nm. This value agrees well with that of a direct determination using transmission electron microscopy on analogous samples [16]. In the Mössbauer spectra, however, the doublet character is more pronounced in the present work than in literature where the reported spectra were obtained with 9.6 nm particles. This reveals a larger fraction of unreduced iron in the present Fe/KL sample. Beside the superparamagnetism as main magnetic feature of the Fe/KL sample also paramagnetism contributes to the magnetic behavior. The paramagnetic contribution is evidenced by the linear increase of the χ (H) curve when the superparamagnetic saturation field of about 10 kOe is exceeded (Fig. 6). The paramagnetic contribution can be assigned to Fe^{2+} and Fe^{3+} ions which were also found by Mössbauer spectroscopy. These ions must be located in the channels of KL zeolite were they cannot interact with each other to form superparamagnetic or antiferromagnetic phases. The amount of paramagnetic iron in reduced Fe/KL

samples can be estimated from the slope of the linear part of the magnetization curve M (H). A Curie constant of 0.9 emu K mol^{-1} compared with 0.7 emu K mol^{-1} for calcined Fe/KL indicates that of the paramagnetic fraction is conserved or even slightly increased during reduction. This confirms that reduction converts mostly the antiferromagnetic particles on the crystallite surface.

3.3. Reduced Pt-Fe/KL

SQUID magnetization measurements performed by varying the temperature at constant fields are shown in Fig. 5 and magnetization measurements in dependence of the field at constant temperature are depicted in Fig. 7. The magnetic behavior is again mainly superparamagnetic as it is evidenced by the high

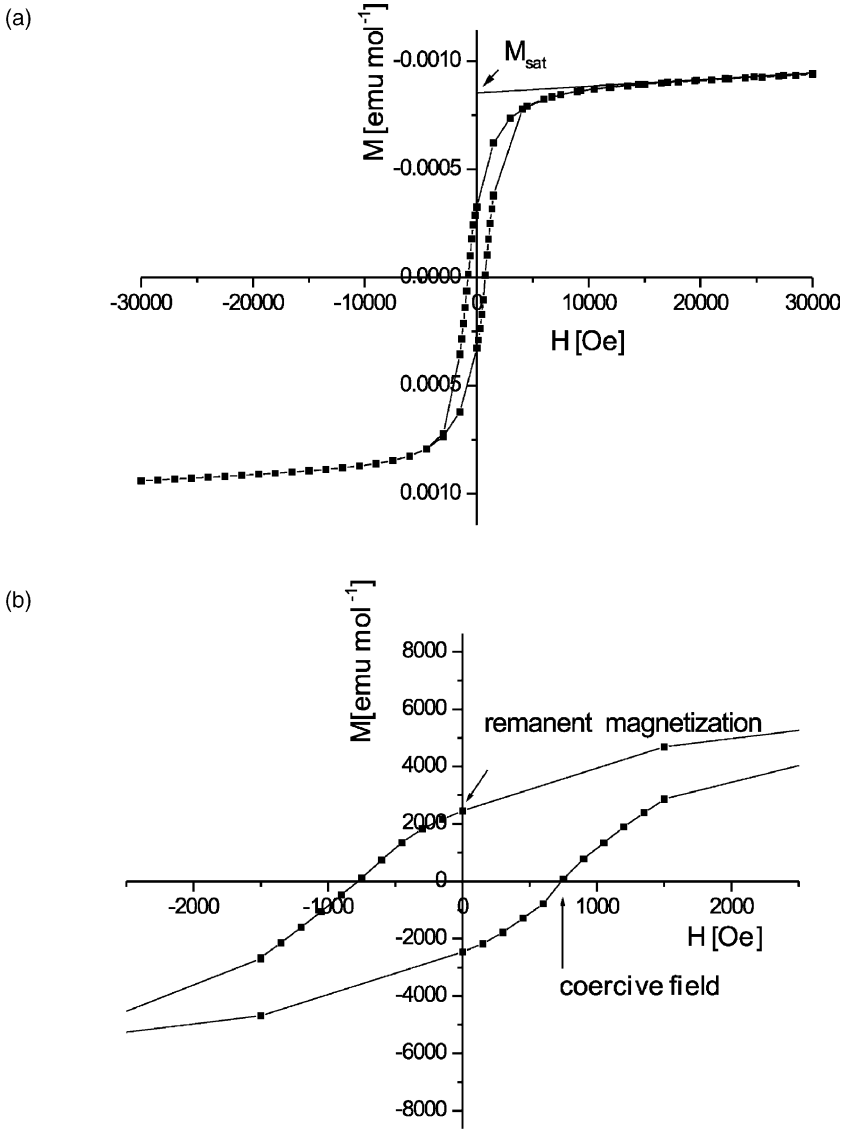

Fig. 7. Molar magnetic susceptibility vs. magnetic field (hysteresis loop) at 50 K of reduced 1.0% Pt-0.3% Fe/KL for a large range (a) and a small range (b).

magnetization and the small remanent magnetization and the small coercive field. Compared to Fe/KL, the saturation magnetization is enhanced by a factor 4, and also the hysteresis loop is slightly larger. According to the Mössbauer data the amount of non-alloyed iron seems to be roughly the same in Fe/KL and in Pt-Fe/KL, but according to the magnetization measurements in the presence of Pt there is clearly an additional superparamagnetic fraction which gives rise to the increased saturation magnetization. Therefore we conclude that the bimetallic catalysts contains small metallic Pt–Fe alloy particles. According to literature [31–36] one of the Mössbauer doublets assigned traditionally to Fe^{3+} should be associated with small Pt–Fe alloy particles. Zheng et al. [16] found a diameter of Pt or Pt–Fe (they were not able to differentiate between these two cases) particles of 2.1 nm. These small particle sizes are well consistent with the present result that Pt–Fe behaves superparamagnetic, but not ferromagnetic. Probably there is a distribution of particle sizes and the enlargement of the coercive field can be explained the influence of a small fraction of larger ferromagnetic Pt–Fe particles, however, the largest fraction of Pt–Fe alloy particles is superparamagnetic. The saturation magnetization of bulk Pt–Fe (1:1 stoichiometry) is 19,100 emu mol^{-1} [50]. This value is higher than the saturation magnetization of monometallic Fe (4904 emu mol^{-1}), and as in the case of calcined samples this can be explained by spin orbit coupling between Fe and Pt [51]. Although, the exact stoichiometry of Pt–Fe alloy particles in samples is unknown it seems reasonable that the magnetization of 4904 emu mol^{-1} corresponds to about 25% of the total iron in reduced Pt-Fe/KL. Due to this strong evidence obtained from SQUID magnetization measurements, it seems reasonable that one of the Mössbauer signals in the isomer shift range between 0.3 and 0.4 mm s^{-1} must be assigned to Pt–Fe alloy particles. This result confirms the conclusions of Schünemann et al. [35] who proved for the first time unambiguously that the Mössbauer signal of a Rh-Fe/NaY catalyst is due to Fe(0), although its chemical isomer shift is similar to that of Fe^{3+}. As in the work of other authors [29,31–33] the comparison of the Mössbauer results by another method gives strong evidence for a Pt–Fe alloy phase. Some other authors found Mössbauer signals with an isomer shift of 0.11–0.16 mm s^{-1} [22] and 0.07 mm [23],

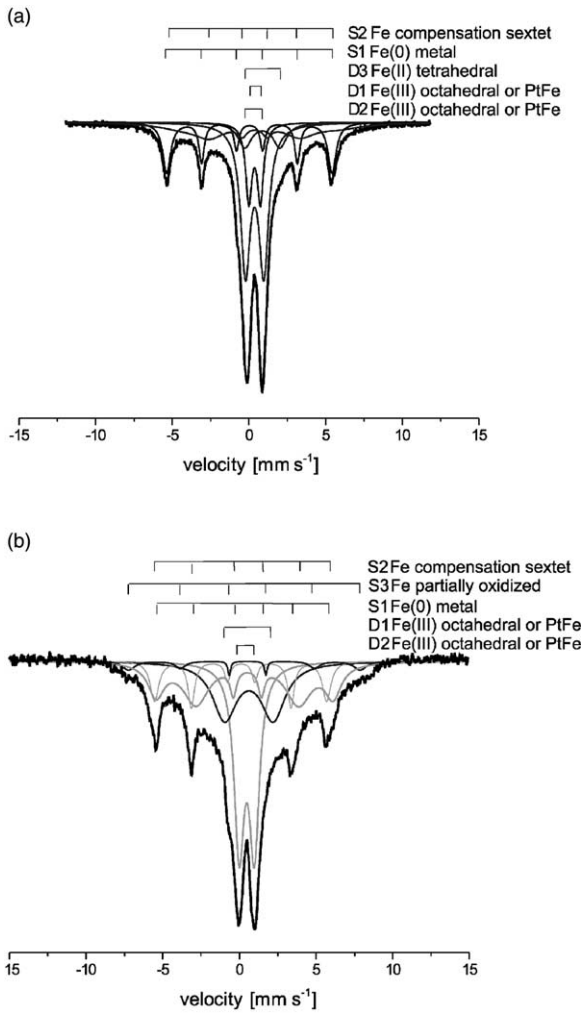

Fig. 8. Mössbauer spectra of reduced 1.0% Pt-0.3% Fe/KL at (a) 295 K, (b) 78 K.

respectively that they assigned to Pt–Fe alloy phases. These isomer shifts are common for bulk Pt–Fe alloy phases, and one may think that this is in contradiction to the results of this work. On the other hand, the isomer shift is a result of the electronic environment surrounding the ^{57}Fe nucleus. In a Pt–Fe alloy phase, this should be strongly dependent on the electric charge of a Pt–Fe particle and on the molar ratio of Pt/Fe. Furthermore, it should be different for a ^{57}Fe nucleus inside an alloy particle from that of a ^{57}Fe nucleus on the surface of an alloy parti-

Table 5
Mössbauer parameters of reduced 1% Pt-0.3% Fe/KL at 295 and 78 K and their assignments (D: doublet, S: sextet)

	78 K				295 K			
	IS ($mm\,s^{-1}$)	QS ($mm\,s^{-1}$)	HF (T)	signal area (%)	IS ($mm\,s^{-1}$)	QS ($mm\,s^{-1}$)	HF (T)	Signal area (%)
Dl Fe(III) octahedral or Fe(0) in Fe–Pt alloy	0.48	0.99		30.79	0.37	0.75		12.88
D2 Fe(III) octahedral or Fe(0) in Fe–Pt alloy	0.62	3.16		22.91	0.37	1.19		38.11
D3 Fe(II) tetrahedral					0.88	2.29		8.96
S1 Fe(0) metal	0.10	−0.04	34.9	12.52	0.03	−0.01	33.5	20.39
S2 Fe partially oxidized	0.43	−0.21	46.9	3.82				
S2 Fe(III) compensation sextet	0.43	−0.18	35.9	29.96	0.57	0.38	31.6	19.66

IS: isomer shift, OS: quadrupole splitting, HF: hyperfine splitting.

cle [32]. Mössbauer spectra of reduced Pt-Fe/KL catalyst were recorded at 295 and 78 K and are shown in Fig. 8 and the Mössbauer parameters are summarized in Table 5.

As in the case of reduced Fe/KL samples, the paramagnetic fraction is left mainly unaffected, and in conclusion mainly iron oxides on the outer shell were reduced to alloyed Pt–Fe and unalloyed Fe particles. On the other hand, it is reported that most active for catalysis are not Pt clusters on the outer surface, but clusters located in the zeolite channels [52,53]. This points out that, although bimetallic Pt–Fe clusters are formed, this cannot be the main reason for an improved sulfur resistance.

The amount of superparamagnetic saturation magnetization is not the only property that changes between Fe/KL and Pt-Fe/KL catalysts. Mössbauer spectroscopy reveals that the coordination geometry for Fe^{2+} ions changes from octahedral for Fe/KL samples to tetrahedral for Pt-Fe/KL catalysts. Thus, it should be concluded that the coordination geometry of Fe^{2+} ions is influenced by the presence of Pt, and therefore such that Fe^{2+} ions and clusters are in direct contact. The effect of this interaction between Fe and Pt might be the anchoring of metallic Pt–Fe and Pt clusters by Fe^{2+} ions to the zeolite framework. This inhibits further aggregation and was proposed to be responsible for the enhanced resistance of Pt-Fe/KL catalysts against sulfur poisoning [10,11]. It seems likely that this is the key factor for obtaining a high sulfur resistance.

4. Conclusions

The state of iron in Fe/KL and Pt-Fe/KL samples has been investigated. The characteristic properties and the mutual influence of Fe and Pt can be described as follows:

1. Only Fe^{3+} ions were found after calcination of both, Fe/KL and Pt-Fe/KL catalysts. A fraction with a lower limit of 35–40% occurs as isolated spins and shows paramagnetic behavior, corresponding to iron ions dispersed atomically or as very small aggregates in the channels of the zeolite. The rest is attributed to somewhat larger antiferromagnetic iron oxide particles located mostly at the outer surface of the zeolite crystallites. In the presence of Pt the paramagnetic fraction was slightly higher, but this may only reflect the limits of reproducibility of the sample preparation.
2. Reduction leaves the paramagnetic fraction mainly unaffected, which agrees with an earlier report stating that hydrogen cannot reduce isolated iron ions which are stabilized by the zeolite framework [14].
3. Hydrogen reduces the Fe_2O_3 particles at the outer surface mostly to metallic iron, but some of it remains partly oxidized as Fe^{2+}. These reduced particles have a superparamagnetic or at 50 K to some extent ferromagnetic character with a small hysteresis loop. The magnetic parameters are compatible with a particle diameter of ca. 2.5 nm which agrees well with an earlier direct determination on similar samples [16].

4. The presence of Pt has a pronounced influence on the magnetic properties of the particles on the crystallite surface. The saturation magnetization, the coercive field and in particular the remanent magnetization are considerably larger, an effect that is known also from bulk Pt–Fe alloys. It reflects clearly an electronic interaction between the two elements by which Fe acquires more orbital momentum. These results show that metallic Pt–Fe alloy particles are formed in bimetallic catalysts, and consequently one of the Mössbauer signals similar to Fe^{3+} must be assigned to Fe(0). This confirms therefore the conclusions of Schünemann et al. [35]. Due to the fact that particles on the crystallite surface are less active than particles in the zeolite channels for catalysis [52,53] it seems unlikely that this interaction is of relevance for the enhanced sulfur resistance of Pt-Fe/KL in comparison to plain Pt/KL.
5. Some Fe^{3+} ions are reduced to Fe^{2+}. The coordination geometry is influenced by the presence of Pt. Unlike the formation of larger Pt–Fe alloy particles, this effect is not restricted to the outer surface. It therefore seems very likely that the anchoring of small Pt clusters to the zeolite framework by Fe^{2+} ions is responsible for the enhanced sulfur resistance.

Acknowledgements

We thank CU Chemie Uetikon AG in Uetikon/Switzerland for providing KL zeolite for our research, we thank the 2. Physikalisches Institut der Universität Stuttgart for giving us access to their SQUID device and M. Vidal and H.-J. Kümmerer for introducing us to the instrument, B. Pilawa for useful discussions and J. Zheng for help concerning the preparation of samples. We acknowledge financial support by the Deutsche Forschungsgemeinschaft through the Graduate College no. 448 (Modern Magnetic Resonance Type Methods in Materials Science).

References

[1] T.R. Hughes, W.C. Buss, P.W. Tamm, R.L. Jacobson, Stud. Surf. Sci. Catal. 28 (1986) 725.
[2] J. Zheng, J.L. Dong, Q.H. Xu, Appl. Catal. 126 (1995) 141.
[3] P.W. Tamm, D.H. Mohr, C.R. Wilson, Stud. Surf. Sci. Catal. 38 (1987) 335.
[4] M. Vaarkamp, J.T. Miller, F.S. Modica, G.S. Lane, D.C. Koningsberger, J. Catal. 1238 (1992) 675.
[5] G.B. McVicker, J.L. Kao, J.J. Ziemiak, W.E. Gates, J.L. Robbins, M.M.J. Treecy, S.B. Rice, T.H. Vanderspurt, V.R. Cross, A.K. Ghosh, J. Catal. 157 (1993) 48.
[6] L.J. Simon, J.G. Van Ommen, A. Jentys, J.A. Lercher, J. Catal. 201 (2001) 60.
[7] M. Guenin, M. Breysse, R. Frety, K. Tifouti, P. Marecot, J. Barbier, J. Catal. 105 (1987) 144.
[8] G. Connell, J.A. Dumesic, J. Catal. 101 (1986) 103.
[9] J.K. Lee, H.K. Rhee, J. Catal. 177 (1998) 208.
[10] W.M.H. Sachtler, Catal. Today (1993) 419.
[11] M.S. Tzou, B.K. Teo, W.M.H. Sachtler, J. Catal. 84 (1994) 1641.
[12] V. Schünemann, H. Treviño, G.D. Lei, D.C. Tomczak, W.M.H. Sachtler, K. Fogash, J.A. Dumesic, J. Catal. 153 (1995) 144.
[13] L. Guczi, Catal. Rev. Sci. Eng. 23 (1981) 329.
[14] K. Lázár, L.F. Kiss, S. Pronier, G. Onyestyák, H.K. Beyer, in: M. Miglierini, D. Peridis (Eds.), Mössbauer Spectroscopy in Materials Science, NATO Science series: 3, Kluwer Academic Publishers, Dordrecht, 1999, p. 291.
[15] H.-Y. Chen, W.M.H. Sachtler, Catal. Today 42 (1998) 73.
[16] J. Zheng, T. Schmauke, E. Roduner, J.L. Dong, Q.H. Xu, J. Mol. Catal. A: Chem. 171 (2001) 181.
[17] R.T. Sanderson, Chemical Binds and Bond Energy, 2nd ed., Academic Press, New York, 1976.
[18] W.J. Mortier, J. Catal. 55 (1978) 138.
[19] O.C. Kistner, A.W. Sunyar, Phys. Rev. Lett. 4 (1960) 229.
[20] P. Gutlich, R. Link, A. Trautwein, Mössbauer Spectroscopy and Transition Metal Chemistry, Springer, Berlin, 1978, p. 44.
[21] W.N. Delgass, in: I.J. Gruverman, C.W. Seidel (Eds.), Mössbauer Effect Methodology, vol. 10, Plenum Press, New York, 1976.
[22] H.S. Woo, T.H. Fleisch, H.C. Foley, S. Uchiyama, W.N. Delgass, Catal. Lett. 4 (1990) 93.
[23] Z. Kajcsos, K. Lázár, G. Brauer, J. Phys. Colloque C4 3 (1993) 197.
[24] Y. Minai, T. Fukushima, M. Ichikawa, T. Tominage, J. Radioanal. Nucl. Chem. Lett. 87 (1984) 189.
[25] J.W. Niemantsverdriet, A.M. van der Kraan, J.J. Loef, W.N. Delgass, J. Phys. Chem. 87 (1983) 1292.
[26] J.W. Niemantsverdriet, D.P. Aschenbeck, F.A. Fortunato, W.N. Delgass, J. Mol. Catal. 25 (1984) 285.
[27] J.W. Niemantsverdriet, A.M. van der Kraan, W.N. delgass, J. Catal. 89 (1984) 138.
[28] J.W. Niemantsverdriet, J.A.C. van Kaam, C.F.J. Flipse, A.M. van der Kraan, J. Catal. 96 (1985) 58.
[29] J.W. Niemantsverdriet, A.M. van der Kraan, Surf. Interface Anal. 9 (1986) 221.
[30] A. Fukuoka, T. Kimura, N. Kosugi, H. Kuroda, Y. Minai, Y. Sakai, T. Tominaga, M. Ichikawa, J. Catal. 126 (1990) 434.
[31] R.L. Garten, in: I.J. Gruvernab (Ed.), Mössbauer Effect Methodology, vol. 3, Plenum, New York, 1976, p. 69.
[32] Y.L. Lam, R.L. Garten, in: Proceedings of the 6th Ibero-American symposium on Catalysis, Rio de Janeiro, 1978.

[33] M.A. Vannice, Y.L. Lam, R.L. Garten, Adv. Chem. 178 (1979) 15.
[34] R.L. Garten, J.H. Sinfelt, J. Catal. 62 (1980) 127.
[35] V. Schünemann, H. Treviño, W.M.H. Sachtler, K. Fogash, J.A. Dumesic, J. Phys. Chem. 99 (1995) 1317.
[36] L. Xu, G. Lei, W.M.H. Sachtler, R. Cortright, J.A. Dumesic, J. Phys. Chem. 97 (1993) 11517.
[37] V.R. Balse, W.M.H. Sachtler, J.A. Dumesic, Catal. Lett. 1 (1988) 275.
[38] D. Palaith, C.W. Kimball, R.S. Preston, J. Crangle Phys. Rev. 178 (1969) 93.
[39] J.H.A. Martens, R. Prins, J.W. Niemantsverdriet, J. Catal. 108 (1987) 259.
[40] M.A. Vannice, R.L. Garten, J. Mol. Catal. 1 (1975/76) 201.
[41] C.H. Bartholomew, M. Boudart, J. Catal. 29 (1973) 278.
[42] J.B. Goodenough, W. Gräper, F. Höltzberg. D.L. Huber, R.A. Lefever, J.L. Longer, T.R. Mc.Guire, S. Methfessel, Landot-Bomstein, Group III: solid materials, in: K.-H. Hellwege, A.M. Helwege (Eds.), Magnetic and Other Properties of Oxides and Related Compounds, vol. 4a, Springer, Berlin, Heidelberg, New York, 1970.
[43] S. Gangopadhyay, G.C. Hadjipanayis, B. Dale, C.M. Sorenson, K.J. Klabunde, V. Papaefthymiou, A. Kostikas, Phys. Rev. B 45 (1992) 9778.
[44] T.W. Richards, G.E. Behr Jr., Z. Phys. Chem. 58 (1907) 303.
[45] J. Zheng, J.L. Dong, Q.H. Xu, Stud. Surf. Sci. Catal. 84 (1994) 1641.
[46] J. Zheng, J.L. Dong, Q.H. Xu, C. Hu, Catal. Lett. 37 (1996) 25.
[47] P.A. Jacobs, Stud. Surf. Sci. Catal. 29 (1986) 357.
[48] D. Goldfarb, M. Berbardo, K.G. Strohmaier, D.E.W. Vaughan, H. Thomann, J. Am. Chem. Soc. 116 (1994) 6344.
[49] D.E. Gray, American Institute of Physics handbook, 3rd ed., McGraw-Hill, New York, 1972.
[50] B. Bian, D.E. Laughlin, K. Sato, Y. Hirotsu, J. Appl. Phys. 87 (2000) 6962.
[51] N.D. Van, The Influence of Ag- and Mo-Doping on Magnetic Properties of Fe-Pt Thin Films, Master Thesis, International Training Institute for Material Science, Hanoi, 2001.
[52] C.M. M'Kombe, M.E. Dry, C.T. O'Connor, Zeolites 19 (1997) 175.
[53] M.M.J. Treacy, Microporous Mesoporous Mater. 28 (1999) 271.